

## REVIEW

# Remotely sensed surrogates of meteorological data for the study of the distribution and abundance of arthropod vectors of disease

By S. I. HAY

*Trypanosomiasis and Land-use in Africa (TALA) Research Group, Department of Zoology, University of Oxford, South Parks Road, Oxford OX1 3PS, U.K.*

C. J. TUCKER

*NASA, Goddard Space Flight Centre, Earth Resource Branch, Code 923, Greenbelt, MD 20771, U.S.A.*

D. J. ROGERS AND M. J. PACKER

*Trypanosomiasis and Land-use in Africa (TALA) Research Group, Department of Zoology, University of Oxford, South Parks Road, Oxford OX1 3PS, U.K.*

*Received 20 September 1995, Accepted 21 September 1995*

---

This paper gives an overview of how certain meteorological data used in studies of the population dynamics of arthropod vectors of disease may be predicted using remotely sensed, satellite data. Details are given of the stages of processing necessary to convert digital data arising from satellite sensors into ecologically meaningful information. Potential sources of error in these processing steps are also highlighted. Relationships between ground-measured meteorological variables (saturation deficit, ground temperature and rainfall) and data from both the National Oceanic and Atmospheric Administration's, polar-orbiting, meteorological satellites and the geostationary, Meteosat satellite are defined and examples detailed for Africa. Finally, the current status of existing satellite platforms and future satellite missions are reviewed and potential data availability discussed. How such satellite-based predictions have proved valuable in understanding the distribution of tsetse fly species in Côte d'Ivoire and Burkina Faso will be the subject of a future review.

## INTRODUCTION

### Vector Biology and Climate

Many arthropod vectors of parasites are sensitive to climate, which is generally expressed as temperature, humidity or saturation deficit and rainfall (Nash, 1933; Buxton and Lewis, 1934; Bursell, 1957, 1958, 1959; Rogers and Randolph, 1991). Each of these factors may directly affect the birth, death or migration rates of the vectors and thus may indirectly

affect population sizes. This applies to both the long-term equilibrium values (determined by the interaction of the long-term, average, climate-related or abiotic mortalities with density-regulating processes in the life cycle) and the shorter-term changes around such equilibria (determined by the sensitivity of the equilibria to short-term fluctuations in climate). The importance of climate and its short-term manifestation, weather, to insect-borne disease is highlighted in the standard

formula for the basic reproductive rate or number of such diseases,  $R_0$ , given by:

$$R_0 = \frac{a^2 m c b e^{-\mu T}}{\mu r}$$

where  $a$  is the the vector biting rate,  $m$  the ratio of vectors to hosts,  $c$  the transmission coefficient from vertebrate to vector (i.e. the proportion of bites by vectors on infected hosts that eventually give rise to mature infections in the vectors),  $b$  the transmission coefficient from vector to vertebrate,  $\mu$  the vector mortality rate,  $T$  the incubation period of the infection within the vector and  $r$  the rate of recovery of the vertebrate from infection (Rogers, 1988). In this generalized equation, six of the seven parameters or variables are some function of the vector and only one ( $r$ ) is a function of the host alone. Given the importance of many aspects of vector biology and behaviour to the transmission of vector-borne diseases, it must follow that the distribution and intensity of such diseases is often dependent upon the distribution and abundance of the vectors, which in turn depends upon climate.

Weather is usually measured at ground level, in Stevenson screens, as maximum and minimum temperatures, relative humidity, precipitation, and occasionally, sunshine hours. Synoptic (long-term average) weather measurements are published as climate tables and may form the basis for studies of the impact of climate on vectors (Nash, 1933; Buxton and Lewis, 1934; Rogers and Randolph, 1986). There are, however, several problems with this approach. Firstly, it is unlikely that a weather station contributing to the published data sets is located where the vector studies are carried out. Secondly, the climate records are of long-term averages, whilst researchers often want to relate contemporary weather and vector demography. Thirdly, even if it exists at the study site, a weather station is unlikely to record conditions in the microhabitats where vectors spend most of their time.

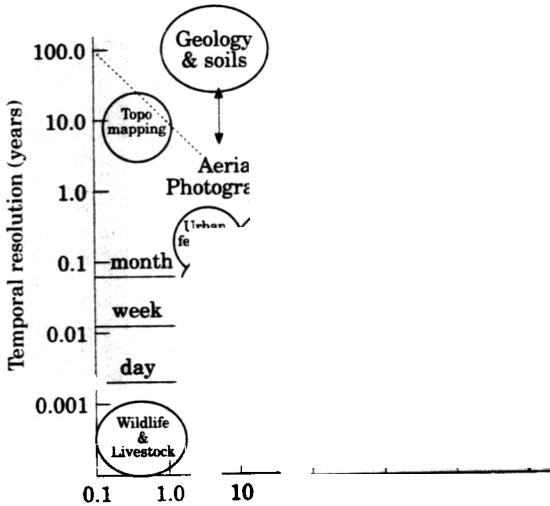
Several solutions to these problems are available. Firstly, interpolation between fixed, meteorological site records can produce climate surfaces, from which conditions at any

particular study site can be read. Various interpolation routines have been tested and those currently used claim an accuracy of 95% for points distant from climate stations with a sufficient density and spread of recording stations (Lennon and Turner, 1995). Secondly, daily weather data may be obtained from archives. Thirdly, researchers may run their own weather stations. None of these solutions is entirely satisfactory, however, and each has further problems. For example, meteorological stations may be at too low a density and/or too irregularly distributed for interpolation regimes to give satisfactory predictions. Furthermore, it may not be possible to extend an analysis based on a project's own daily meteorological data to a regional level without running into the first two problems once again.

In recent years, satellites have been viewing the Earth, in a number of wavebands in the visible and infra-red regions of the electromagnetic spectrum, and the data they collect have been related to synoptic and contemporary, ground-based measurements of climate or weather (Rogers and Randolph, 1991). In this review, we show how such data can overcome the first two of the three problems mentioned above and ameliorate the third, and how, therefore, they may contribute to both large- and small-scale studies (i.e. small- and large-area studies, respectively) of arthropod vectors of the diseases of man and other animals. A second paper (Rogers *et al.*, 1996) will show how processed satellite data have been used to interpret the distribution and abundance of several species of tsetse fly in Côte d'Ivoire and Burkina Faso. Previous applications of remotely sensed imagery to studies of vector-borne disease have been reviewed by Cline (1970), Hugh-Jones (1989) and Washino and Wood (1994).

### Remote-sensing Platforms

Remote-sensing satellites are of two broad categories: geostationary; and polar-orbiting. Geostationary satellites are put into an orbit at the equator, with a speed equal to that of the Earth's rotation, to keep them above a fixed point on Earth. The onboard sensors view the Earth as a disc, so that, apart from spherical



distortion, there are few, if any, problems of registering such images to base maps.

Polar-orbiting satellites circle the globe repeatedly, which means that successive orbits pass over a different section of the rotating Earth. The swath-width of sensors or radiometers on board such satellites is determined by the satellite altitude and sensor characteristics, resulting in the repeat time (the time between viewing the same part of the Earth's surface) varying between satellite systems. The raw data or images from polar-orbiting satellites are a series of strips which must be co-registered and geometrically corrected before successive images can be joined together. Images are stored and transmitted as digital data, each value being a picture element or 'pixel' that refers to a small area in the satellite sensor's field of view. Any given pixel represents the aggregate spectral signal from all objects within the pixel bounds.

Satellite images are limited in their spectral, spatial and temporal resolutions by a variety of

factors, reflecting a compromise between the constraints of atmospheric effects, engineering limitations and the desired, end-user application. The signal that satellites receive of the Earth has passed through an atmosphere whose transmission characteristics are variably affected by gases, aerosols, dust and moisture. Water vapour especially renders the atmosphere opaque in a large part of the electromagnetic spectrum and passive satellite sensors can only operate within atmospheric 'windows' between these opaque regions. Within each window, the viewing sensors may have broad or narrow specificities (i.e. they are able to detect a broad or narrow range of wavelengths), unalterably determined at design-time.

The compromise between the spatial and temporal resolutions of satellite images is illustrated in Fig. 1, in which the dashed line represents a fixed volume of image data. Given that satellite data volume is often limited by on board, image-storage facilities (especially in

TABLE

The spectral, spatial and temporal resolution of the 'satellite pour l'observation de la terre' (SPOT), High Resolution Visible (HRV); Landsat, Thematic Mapper (TM); National Oceanic and Atmospheric Administration (NOAA), Advanced Very High Resolution Radiometer (AVHRR) and Meteosat, High Resolution Radiometer (HRR)

| Satellite/Radiometer | Resolution  |  |            |
|----------------------|---|--|------------|
|                      | Spectral*   | Spatial†   | Temporal   |
| SPOT/HRV             | Channel 1 (panchromatic; 0.51–0.73)<br>Channel 2 (multispectral; 0.50–0.59)<br>Channel 3 (multispectral; 0.61–0.68)<br>Channel 4 (multispectral; 0.79–0.89)                   | 10 m (panchromatic)<br>or 20 m (multispectral)   | 26 days‡   |
| Landsat/TM§          | Channel 1 (0.45–0.52)<br>Channel 2 (0.52–0.60)<br>Channel 3 (0.63–0.69)<br>Channel 4 (0.76–0.90)<br>Channel 5 (1.55–1.75)<br>Channel 6 (2.10–2.35)<br>Channel 7 (10.40–12.50) | 30 m (channels 1–6)<br>or 120 m (channel 7)      | 16–18 days |
| NOAA/AVHRR           | Channel 1 (0.58–0.68)<br>Channel 2 (0.72–1.10)<br>Channel 3 (3.55–3.93)<br>Channel 4 (10.30–11.30)<br>Channel 5 (10.50–11.50)   | km   |            |
| Meteosat/HRR         | Channel 1 (0.40–1.10)<br>Channel 2 (10.50–12.50)<br>Channel 3 (5.70–7.10)   | 2.4 km (channel 1)<br>or 5 km (channels 2 and 3) | 0.5 h      |

\*The spectral resolutions are the electromagnetic wavelengths in  $\mu\text{m}$ , where 0.4  $\mu\text{m}$  is at the blue end of the spectrum and 0.6  $\mu\text{m}$  at the red.

†Spatial resolution is given as the instantaneous field of view of the sensor at nadir.

‡A pointing facility can improve the frequency of coverage at an additional cost.

§An additional instrument, the Multispectral Scanner (MSS) can provide data in 5 bands at 82 m resolution.

older satellites) and the limited opportunity for telemetry (transmission of data between satellite and receiving station) during the satellite overpass, remotely sensed images tend to have either high-temporal or high-spatial resolution, but not both. The figure shows the compromises reached between spatial and temporal resolutions by the current collection of Earth-orbiting satellites. In general, the satellites with high spatial resolution, of the Landsat multi-spectral-scanner (MSS) and thematic-mapper (TM) series and the 'satellite pour l'observation de la terre' (SPOT) series (see Table for details), give finely detailed images, with pixel sizes down to 30 or 10 m (Landsat TM and SPOT panchromatic, respectively)

but with repeat-times of approximately 16 and 26 days, respectively. Frequent cloud contamination of the images means that such satellites give few clear images of the Earth's surface each year, especially over tropical regions. They cannot, therefore, be used to monitor seasonal phenomena, although an average or synoptic picture of seasonality may be built up over several years. In our view, this, together with the high cost of such imagery, generally limits the biological application of high-spatial-resolution imagery to the production of habitat maps for relatively small areas.

In contrast to Landsat and SPOT, the National Oceanographic and Atmospheric Administration (NOAA) series of polar-

orbiting, meteorological satellites each complete 14.1 Earth orbits/day, with a sensor swath-width of about 2700 km, giving two global-coverage images/24-h period (Kidwell, 1995). The spatial resolution from the satellites' advanced, very-high-resolution radiometers (AVHRR) is 1.1 km beneath the track of each orbiting satellite. The 'very-high-resolution' refers to the sensor radiometric resolution rather than its spatial resolution. The spatial resolution reduces with distance along and across the track, due to parallax and the Earth's curvature. Nominal 1.1-km AVHRR data are continuously transmitted and may be received by stations along or near to the satellite's path, when they are referred to as high resolution picture transmission (HRPT) data. On request to NOAA, these 1.1-km data may also be recorded on an on board, tape-storage system and later transmitted to Earth as the satellites pass over a network of receiving stations. The data are then referred to as local area coverage (LAC) data (Hastings and Emery, 1992).

Two processing steps reduce further the spatial resolution of most of the AVHRR data available to the user community. The on board tape system is incapable of holding global coverage data at 1.1-km resolution. Instead, the information from each area of five (cross-track) by three (along-track) pixels is stored as a single value, the average of the first four pixels only of the first row of the  $5 \times 3$  block. The resulting imagery is referred to as global area coverage or GAC data. GAC data, with a stated nominal resolution of  $4 \times 4$  km, are obviously far from ideal representations of the raw data (Justice *et al.*, 1989) and their method of subsampling has consequences for environmental modelling (Belward and Lambin, 1990; Belward, 1992). Nevertheless, GAC data are the form in which most of the AVHRR archive was collected. NOAA satellites have been operational since 1978 and global datasets of reasonable quality are available at a variety of resolutions (GAC or poorer) from the early 1980s to date (Townshend, 1994).

The high-temporal-resolution imagery of the geostationary Meteosat (30 min between picture transmissions) is associated with an

even lower spatial resolution of 2.5–5 km (depending on waveband, see Table), although this is relatively unimportant for large-area, weather-forecasting purposes.

NOAA and Meteosat images are the only data currently available for monitoring seasonal changes in real time and thus have potential for a number of biological applications. Despite the fact that neither satellite series was designed with land-surface studies in mind, over the last few years data from both series have been related to important land-surface phenomena (Goward *et al.*, 1994), including vegetation activity and rainfall. These applications are briefly reviewed below. A general background to remote-sensing applications is given by Swain and Davis (1978), Colwell (1983), Curran (1985), Cracknell and Hayes (1991), Prince *et al.* (1991), Barrett and Curtis (1992) and Lillesand and Kieffer (1994).

### Data Processing

#### IMAGE REGISTRATION TO BASE MAPS

Images derived from satellites are first processed to register them to a base map at a particular scale and in a particular map projection (Snyder, 1987). Registration is generally an automated process that uses an ephemeris model and a time signal sent down with the satellite imagery to predict the satellite's position relative to the Earth at the time of image capture (Emery *et al.*, 1989; Baldwin and Emery, 1993). Algorithms for positional calculations originally assumed that the satellites were in their correct attitude and were following precisely their intended orbits. This is unfortunately not the case (McGregor and Gorman, 1994). Slight deviations from design values, and variations in these deviations, mean that some of the resulting imagery is not precisely registered to the appropriate base maps. Final registration to a base map has therefore to be performed by visual inspection of the image with a map overlay (Krasnopolsky and Breaker, 1994). Image registration to a map tends to involve a loss of spatial resolution, the extent of which is sometimes increased to allow the display of large areas on computer screens with limited spatial resolutions. The effects of these various stages of

image resampling on AVHRR data were considered by Khan *et al.* (1995).

#### MAP PROJECTIONS

AVHRR images produced for famine early-warning systems (FEWS) (Hutchinson, 1991) and the later, Meteosat, cold-cloud duration imagery (see below) with nominal  $7.6 \times 7.6$  km pixel size, are all in the Hammer-Aitoff map projection, which is a linearly re-scaled form of the Lambert azimuthal equal area projection (Snyder, 1987). The re-scaling makes the Hammer-Aitoff no longer azimuthal, points on the map no longer being shown with the correct directions from the centre of projection. The IDA image display software (Pfirman, 1991) that was commissioned by FEWS routinely handles the Hammer-Aitoff projection but commercial software more frequently offers only the Lambert azimuthal projection. Thus, re-projection by the user may be necessary.

#### REMOVAL OF CLOUD CONTAMINATION

Although each of the high-temporal-resolution images from the NOAA (and Meteosat) satellites is as affected by cloud contamination as any single Landsat or SPOT image, their much higher frequency means that good quality results can be obtained by combining images over a relatively short period of time, by compositing. The aim of compositing is to choose the most cloud-free and/or least atmospherically contaminated radiance value within the compositing period. Most compositing algorithms rely on the fact that one common image product from the AVHRR data set, the normalized-difference vegetation index or NDVI, produced from channels 1 and 2 (see below for details), has values that are generally reduced by cloud and other atmospheric contamination (Holben, 1986; Kaufman and Tanré, 1992). The highest NDVI values recorded during any relatively short time period are therefore thought to occur when cloud cover is least and such values are taken to represent the least attenuated pixel value for the period. This method of image production is called maximum value compositing (MVC), and is usually carried out over a 10-day

(‘dekadal’) compositing period. It has the important consequence that maximum image values for adjacent pixels in a single image may have been collected on different days during the compositing period. MVC methods tend to degrade still further the spatial resolution of the final image product, for reasons discussed by Robinson (1996), who concluded that the recorded value for any nominal  $7.6 \times 7.6$  km pixel may in fact have been drawn from an area as large as  $20 \times 20$  km. Other compositing regimes include taking the root mean square value for a given pixel time-series (Kineman *et al.*, 1990) and more sophisticated methods, such as best index slope extraction (BISE) (Viovy *et al.*, 1992). This technique assumes that vegetation grows and senesces over weeks, so that the evolution and decay of the resulting NDVI signal is gradual. Values which lie outside a user-determined threshold from the previous signal are interpolated, as they are probably due to short-term effects of atmospheric contamination.

Selection of the least cloud-contaminated images in the other AVHRR channels usually depends upon the selection of the NDVI value derived by MVC. The same image that is used to generate the NDVI for any pixel is also taken as the source of information for the other AVHRR channels for that pixel and period. Increasingly, however, AVHRR channels 3, 4 and 5 are also being subjected to MVC individually.

#### OTHER ATMOSPHERIC EFFECTS

During image registration to a base map, other corrections for variable atmospheric effects, such as Rayleigh scattering caused by aerosols and absorption by water vapour, CO<sub>2</sub> and ozone, may also be applied, using ancillary information in the satellite data stream (Tanré *et al.*, 1990; Vermote *et al.*, 1990). If corrections for atmospheric effects are not made at the time of image registration they generally cannot be made accurately at a later stage. Instead, corrections are based on average values for a ‘standard’ atmosphere within a region (Hannan *et al.*, 1995).

Despite attempts to remove the effects of clouds and other contaminants by MVC of

AVHRR imagery, continuous, total or partial cloud-cover or residual, thin cloud-cover or haze still affect many products of MVC. Removal of such contamination is the subject of much current research, some of which is referred to below, and has resulted in a proliferation of indices.

#### SATELLITE SENSOR DRIFT

During their operational life-time, the characteristics of the AVHRR sensors change with use and as components age (Gorman and McGregor, 1994). The thermal channels are continuously re-calibrated against the 4°K, space-background temperature. The visible channels are not re-calibrated, however, due to the difficulty of maintaining two standard radiation sources in space (Kidwell, 1995). Sensor 'drift' in the visible channel requires the application of sets of correction factors to indices (e.g. NDVI) that use visible channel data, and these are given by Los (1993).

#### SATELLITE PRECESSION

Even when corrections for atmospheric effects and instrumental drift have been made, however, the resulting imagery may still show periodical changes in the signal, due to a precession of the satellite's orbit. This results in cyclical variation of over-pass times, which in the case of AVHRR imagery have a 17-day cycle (McGregor and Gorman, 1994). Signal variation is then due to the changing angles between the Sun, Earth and satellite sensors.

It is clear, therefore, that the images that are available to the user community may suffer from a variety of defects for many different reasons. Despite these defects, however, correlations between satellite- and ground-based meteorological data can be remarkably good, suggesting that the errors, though not negligible, are small in comparison with the range of data values recorded.

## ANALYSES AND EXAMPLES

### Vegetation

#### VEGETATION INDICES

One of the first land-surface applications of NOAA-AVHRR data was as a vegetation index

to monitor the effects of drought and to forecast potential famine conditions (Hutchinson, 1991). Vegetation indices, reviewed by Huh (1991) and Myneni *et al.* (1995b), exploit the fact that chlorophyll and carotenoid pigments in plant tissues absorb light in the AVHRR channel 1 (visible red) waveband, whereas mesophyll tissue reflects light in the AVHRR channel 2 (near infra-red) waveband (Sellers, 1985; Tucker and Sellers, 1986). A healthy and actively photosynthesising plant will therefore look darker in the visible and brighter in the infra-red region than an unhealthy or dead plant. The early vegetation indices exploited this fact by using the simple ratio of channel 2 ( $Ch_2$ ) over channel 1 ( $Ch_1$ ) reflectances, called the ratio vegetation index (RVI) or simple ratio index (SRI). Later indices attempted to overcome the problem of reflectance from the (usually dark or reddish) soil background by dividing the difference between these two channels by their sum, to give the normalized-difference vegetation index or NDVI:

$$NDVI = \frac{(Ch_2 - Ch_1)}{(Ch_2 + Ch_1)}$$

with values theoretically ranging from -1 to +1 but in practice well within these limits (Colwell, 1974; Tucker, 1979; Tucker *et al.*, 1991). The NDVI, in common with all red/near-infrared indices, is theoretically a specific measure of chlorophyll abundance and energy absorption (Myneni *et al.*, 1995a) but its use has been extended to cover vegetation biomass (Tucker *et al.*, 1983), coverage (Tucker *et al.*, 1985) and phenology (Justice *et al.*, 1985) in a range of ecosystems. NDVI measurements are particularly useful in areas of sparse vegetation coverage, where they have a better dynamic range than the simpler vegetation indices such as RVI. The NDVI does, however, tend to saturate in areas of full coverage, such as forests. It is also less than ideal because of continuing problems with background soils [which are, for example, darkened by rainfall (Huete *et al.*, 1985)] and differential atmospheric effects on the readings in channels 1 and 2 [atmospheric aerosols scatter light particularly in channel 1 whereas atmospheric water vapour

absorbs particularly in channel 2 (Kaufman and Tanré, 1992)].

Alternative indices have been suggested to overcome some of these problems (Jackson and Huete, 1991) but have been less widely applied. The soil-adjusted vegetation index (SAVI) effectively adjusts the intercept of the relationship between channel 2 and channel 1 data to minimize interference from the soil background:

$$SAVI = \frac{Ch_2 - Ch_1}{Ch_2 + Ch_1 + L} (1 + L)$$

$$= \frac{NDVI(1 + L)}{[1 + L/(Ch_2 + Ch_1)]}$$

where  $L$  is a weighting parameter that varies with vegetation coverage. Values for  $L$  of 1.0, 0.75 or 0.25 are recommended for sparse, intermediate and densely vegetated conditions, respectively (Huete, 1988).

More recently, the global-environment monitoring index (GEMI) has been proposed by Pinty and Verstraete (1992), again with the intention of reducing the variability introduced by the soil background and, in addition, of reducing atmospheric effects. Soil effects are minimized because, at least in theory, the GEMI gives a more constant index of vegetation activity against a much wider range of soil conditions than does the NDVI. GEMI was derived from first principles, rather than empirically (although the physical basis for the index is not fully explained in the literature). It is defined as follows:

$$GEMI = \eta(1 - 0.25\eta) - \frac{Ch_1 - 0.125}{1 - Ch_1}$$

where

$$\eta = \frac{2(Ch_2^2 - Ch_1^2) + 1.5Ch_2 + 0.5Ch_1}{Ch_2 + Ch_1 + 0.5}$$

Initial application of GEMI to AVHRR data for Africa indicated that it has three advantages over the NDVI: GEMI is less sensitive to atmospheric variations; it has a much enhanced ability to detect clouds (which appear dark on both NDVI and GEMI but are more easily detected, and may therefore be more easily screened out, by GEMI); and it has a higher

dynamic range in xeric environments, showing details (e.g. of geological formations or land-surface topology) in sparsely vegetated areas that are not visible in other imagery (Flasse and Verstraete, 1994).

#### VEGETATION INDICES AND CLIMATE

Locally, vegetation is influenced by, and affects, both macro- and micro-climatic conditions, especially those related to atmospheric moisture. It is therefore not surprising to find relationships between NDVI and saturation deficit (Rogers and Randolph, 1991). Data presented in the following (and subsequent examples) use mean annual meteorological variables calculated for the period 1941–1970 (Anon., 1983) to assess the accuracy of meteorological predictions based on satellite data. The meteorological stations chosen for comparison were distributed throughout continental Africa, below 24°N. Those stations located near to the coast or adjacent to extensive inland water bodies were excluded from the analysis because the corresponding 7.6 × 7.6 km, remotely sensed pixel could be heavily contaminated by the signal from water. As saturation deficits were not measured directly at the meteorological stations, they were calculated from noon relative humidity and temperature data using a formula given by Unwin (1980). The NDVI values are synoptic annual means for the period 1981–1992. The relationship between saturation deficit and NDVI is linear (Fig. 2) and the strength of the correlation ( $r^2=0.6$ ;  $n=313$ ;  $P \leq 0.001$ ) indicates that the NDVI may be used in studies of arthropod vectors wherever saturation deficit has been useful in the past.

Insect mortality rates are especially sensitive to atmospheric dryness (Bursell, 1957; Platt *et al.*, 1958) and studies on the tsetse fly *Glossina morsitans submorsitans* (Westwood) in Nigeria showed that the correlation between mean monthly fly mortality rates and NDVI was at least as good as that between the same mortality rates and monthly saturation deficit calculated from meteorological records (Rogers and Randolph, 1991). Satellite data therefore seem to be acceptable substitutes for at least some ground-based, meteorological records.

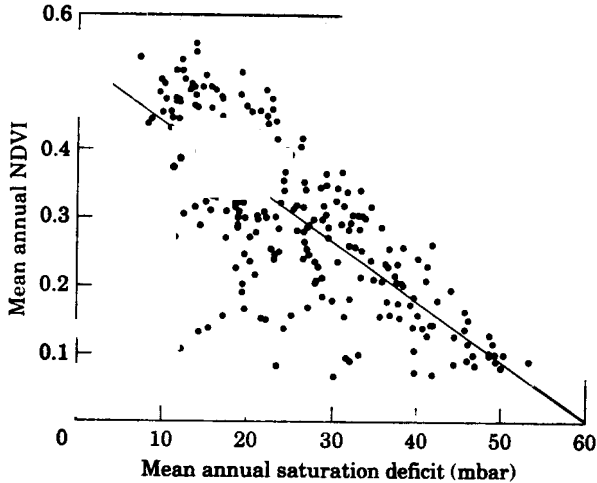


Fig. 2. The relationship between the mean, annual, normalized-difference, vegetation index (NDVI) for the period 1981–1992 and mean, annual, saturation deficit at meteorological stations throughout Africa for the period 1941–1971 ( $r^2=0.61$ ;  $n=313$ ;  $P\leq 0.001$ ).

## Temperature

### THERMAL-BRIGHTNESS TEMPERATURE MEASUREMENTS

All objects above absolute zero emit electromagnetic radiation. The theoretical concept of a black body is used to describe a material that absorbs and emits radiation perfectly at all wavelengths. Such a material has an emissivity coefficient of 1.0. Radiation is emitted by black bodies only as a function of temperature, the relationship formalized in Planck's law (Monteith and Unsworth, 1990). In ideal conditions, therefore, the temperature of a black body can be determined by detecting the energy it emits at a particular wavelength. Natural surfaces, however, do not behave as black bodies and have emissivity values significantly less than 1.0. Furthermore, the thermal-brightness temperature measured by the satellite is also affected by absorption characteristics of atmospheric constituents (particularly water vapour but also ozone,  $\text{CO}_2$  and aerosols), as well as emission of radiation by the atmosphere itself (Vogt, 1992). Attempts to retrieve accurate surface temperatures from satellite-derived brightness temperatures must therefore correct for atmospheric attenuation

and the spatially heterogeneous nature of land-surface emissivity. These are major areas of past and current remote-sensing research (Norman *et al.*, 1995).

Channels 4 and 5 of the AVHRR (both in the infra-red) were designed to measure water-vapour attenuation in the 10–12- $\mu\text{m}$  spectral window for more accurate determination of sea-surface temperatures (Prabhakara *et al.*, 1974). Because the attenuation is greater in channel 5 than in channel 4, the difference in the signal of these two, closely spaced channels can be used to reduce the effects of water-vapour attenuation. This simultaneous use of information from both channels to estimate surface brightness temperatures is described as a 'split-window' technique, because it is performed within the same radiance window of the atmosphere.

Surface emissivity is more variable on land than over the more uniform sea and so allowance should be made for emissivity when comparing surface brightness temperatures of different land-surface types. Price (1984) derived, from radiative transfer theory, the following relationship between surface temperature ( $T_s$ ) and channel-4 and -5 brightness

temperatures ( $T_{b4}$  and  $T_{b5}$ , respectively), which takes into account the emissivity value of the land surface:

$$T_s = T_{b4} + 3.33(T_{b4} - T_{b5}) \left( \frac{3.5 + \varepsilon_4}{4.5} \right) + 0.75T_{b5}(\varepsilon_4 - \varepsilon_5)$$

where  $\varepsilon_4$  and  $\varepsilon_5$  are the emissivities at channel-4 and channel-5 wavelengths, respectively.

This algorithm was later found to be accurate to  $\pm 3^\circ\text{C}$  for a uniform, tallgrass prairie habitat in Kansas, when a constant emissivity was assumed (Cooper and Asrar, 1989). Many other split-window techniques have been developed, which largely rely on ancillary data to quantify atmospheric water content and surface emissivity (Prata, 1993).

#### SURFACE BRIGHTNESS MEASUREMENTS AND HABITAT TEMPERATURES

The view of the land surface that satellite infra-red sensors record is a function of the different brightness temperatures of each object in the environment. This view is also affected by the reflectance of incident solar radiation (which in turn is affected by emissivity), as well as the attenuation of the signal by the continuously changing atmospheric column. It is not at all clear, therefore, how the resulting satellite signals relate directly to standard meteorological variables such as air temperature.

Habitats are composed of differing mixtures of soil, water, air and vegetation, each with differing thermal characteristics and often with different temperatures. All abiotic components would equilibrate to the same temperature under conditions of thermal stability but the cycle of solar irradiation means these conditions are never met and are only approximated at the end of the night-time period. As each morning progresses, the temperature of the air near the ground rises faster than that of the ground itself; in the afternoon it falls faster. The difference between the temperatures of the soil and air results in a flow of thermal energy between them, which produces atmospheric effects resulting in both local and

regional mixing of bodies of air at different temperatures.

During the daily temperature cycle in the tropics, organisms the size of arthropods may encounter temperature variations of  $30^\circ\text{C}$  or more. They often ameliorate this behaviourally by moving between temperatures determined mostly by the soil, air or local vegetation. In the past, demographic rates for arthropod vectors have been related to standard, Stevenson-screen meteorological records (generally of air temperature recorded twice daily, at or near dawn and at noon or in the early afternoon, at a height of 1.1 m above the ground), although how such measurements relate to the conditions actually experienced by the vectors is usually unknown (Nash and Page, 1953).

If we knew whether arthropods were more sensitive to thermal radiation emitted by the surface or to incident radiation from the Sun, it would be clearer which of the AVHRR thermal infra-red channels (5 or 2) is most suitable for monitoring as a potential predictor of the vector's birth and death rates. In general, insects show adaptive thermal behaviour, benefiting from radiation from nearby bodies, or directly from the Sun when it is cold, and reducing heat input and increasing the rate of cooling through radiative or convective losses (rarely evaporative cooling) when it is hot (Willmer and Unwin, 1981; Willmer, 1982). As we do not know the precise balance of thermal gains and losses to insect vectors on a daily or longer-term basis, the choice of an appropriate AVHRR channel remains obscure. At present, all that can be done is to establish the best satellite correlates of contemporary weather or synoptic climate data to determine the efficiency with which satellite data can replace the conventional weather data used previously in vector studies. Later, it may be possible to explore the relationship between the vector's demographic rates and contemporary, thermal infra-red satellite data, independently of ground-based meteorological records, in order to seek better predictors of these rates than are presently available from standard meteorological data.

Figure 3 shows the relationship between mean, annual, AVHRR-channel-4, brightness

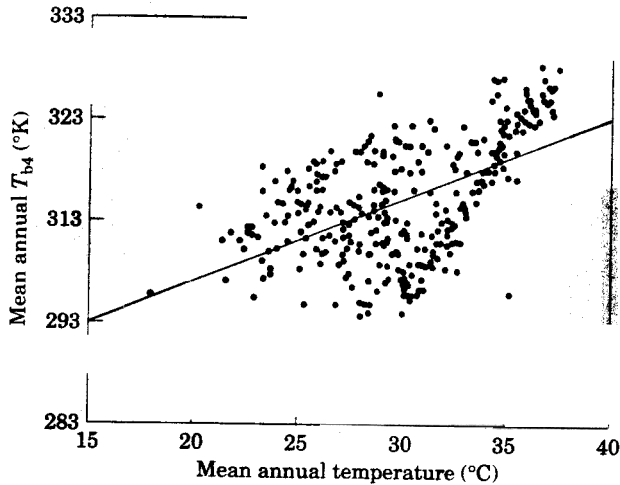


Fig. 3. The relationship between the mean, annual, channel-4 brightness temperature ( $T_{b4}$ ) for the period 1987–1992 and ground air temperature at meteorological stations throughout Africa for the period 1941–1971 ( $r^2=0.31$ ;  $n=351$ ;  $P\leq 0.001$ ).

temperatures and synoptic annual temperatures, again taken from meteorological tables for Africa (Anon., 1983). The AVHRR data were supplied, by the global inventory monitoring and modelling systems (GIMMS) group at the NASA Goddard Space Flight Centre, as  $7.6 \times 7.6$  km resolution, MVC dekads for the period 1987–1992. Since daily data were not available at that time, application of split-window techniques was not possible. A geographical analysis of residuals indicated that the deviations from the regression line were related to altitude. When altitude, derived from a digital elevation surface for Africa provided by the global land information system (GLIS) of the United States Geological Survey (USGS) Earth Resources Observations Systems (EROS) Data Centre was included as an additional predictor variable in a multiple regression, the coefficient of determination increased from  $r^2=0.31$  ( $n=351$ ;  $P\leq 0.001$ ) to  $r^2=0.69$  ( $n=351$ ;  $P\leq 0.0001$ ). The scatter of points is also reduced ( $r^2=0.86$ ;  $n=165$ ;  $P\leq 0.0001$ ) when smaller areas in West Africa (Côte d'Ivoire and Burkina Faso) are investigated using comparisons of monthly meteorological data (see Fig. 4). These relationships have further been shown to be

robust, in a range of habitat types and throughout the year, with African data-sets (Hay, 1993).

## Rainfall

### METEOSAT COLD-CLOUD DURATION

In the tropics, with predominantly convective rainfall, clouds with a cloud-top temperature of less than a threshold value (of about  $-40^\circ\text{C}$ ) are more likely to be rain-bearing than those with higher cloud-top temperatures. These cloud-top temperatures are recorded by the thermal infra-red channel 2 of the Meteosat satellite (Table) that is positioned in geostationary orbit over the Greenwich Meridian at the equator, and so covers Africa, Europe and the Middle East. Similar satellites are operated by the United States (GOES; geostationary operational environmental satellite), Russia (GOMS; geostationary operational meteorological satellite) and Japan (GMS; geosynchronous meteorological satellite) and, together with Meteosat, give global coverage except for the polar regions (Cracknell and Hayes, 1991). The particular threshold temperature associated with rain-bearing clouds and the quantity of rain they deposit varies

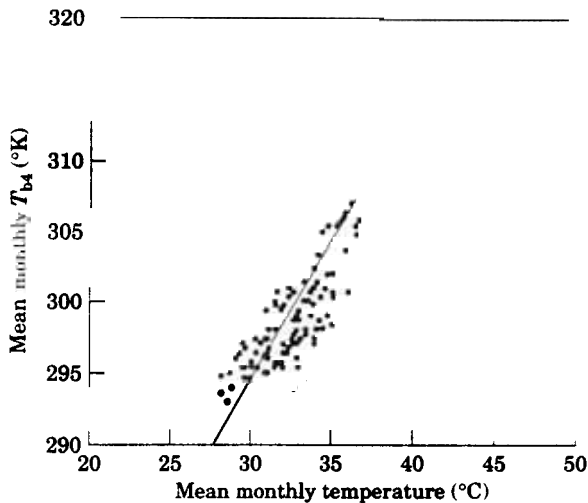


Fig. 4. The relationship between the mean, monthly, channel-4 brightness temperature ( $T_{b4}$ ) for the period 1987–1992 and mean, monthly, ground air temperature at meteorological stations in Côte d'Ivoire and Burkina Faso for the period 1941–1971 ( $r^2=0.86$ ;  $n=165$ ;  $P\leq 0.0001$ ).

temporally and spatially and thus must be established empirically (Milford and Dugdale, 1990). This has been done by the 'tropical applications in meteorology of satellite and other data' (TAMSAT) programme for the area of West Africa from the equator to south of the Sahara desert (Snijders, 1991) and the results are now used by the African, real-time, environmental monitoring and information system (ARTEMIS) of the Food and Agriculture Organization (FAO), Rome, to generate dekadal and monthly images of cold-cloud duration (CCD) (the number of hours for which each pixel was covered by cold clouds during the compositing period) for use in crop monitoring and exercises in forecasting locust plagues (Hielkema, 1990; Anon., 1994). In the production of composite CCD for the whole of Africa, the experimentally determined, threshold cloud-top temperatures are used within the TAMSAT region of Africa (Dugdale *et al.*, 1995) and set thresholds of  $-50^{\circ}\text{C}$  in the summer and  $-60^{\circ}\text{C}$  in the winter or of  $-40^{\circ}\text{C}$  all year round are used for regions north and south of this area, respectively (F. L. Snijders, unpubl. obs.). More sophisticated techniques of rainfall estimation, that relate

cloud-top reflectances and the growth and decay of cloud systems to rainfall amounts, are reviewed by Petty (1995).

#### CCD IMAGERY AND RAINFALL

Figure 5 shows the relationship between monthly mean CCD values for a 5-year period (1988–1992) and synoptic rainfall data for meteorological stations throughout Africa (Anon., 1983). The CCD imagery was supplied by ARTEMIS and covered the whole of Africa at a spatial resolution of  $7.6 \times 7.6$  km. There is a strong positive linear relationship ( $r^2=0.69$ ;  $n=354$ ;  $P\leq 0.001$ ), which is similar ( $r^2=0.62$ ;  $n=132$ ;  $P\leq 0.001$ ) when comparisons are made using monthly data in smaller areas, such as Côte d'Ivoire and Burkina Faso again (see Fig. 6). Furthermore, altitude explained very little of the variance in this relationship, increasing the  $r^2$  value to 0.64 when included as a second variable in a multiple regression. Large spatial variation in rainfall places limits on comparisons of point, rain-gauge data and satellite estimates of rainfall, since rainfall measurements over a season can vary by a factor of two over distances of  $<10$  km (Flitcroft *et al.*, 1989).

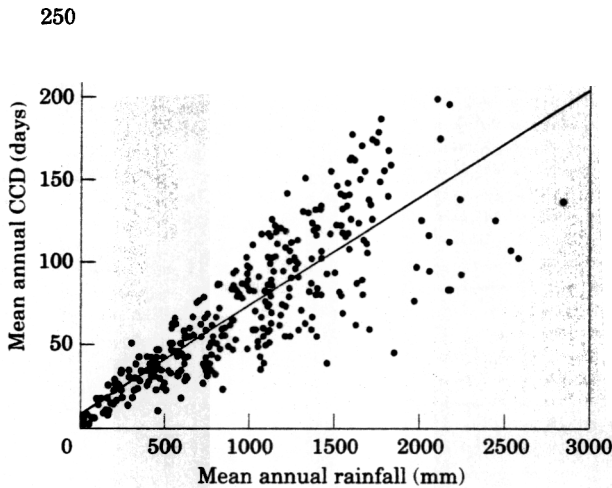


Fig. 5. The relationship between the mean, annual, cold-cloud duration (CCD) for the period 1988–1992 and mean, annual rainfall at meteorological stations throughout Africa for the period 1941–1971 ( $r^2=0.69$ ;  $n=354$ ;  $P \leq 0.001$ ).

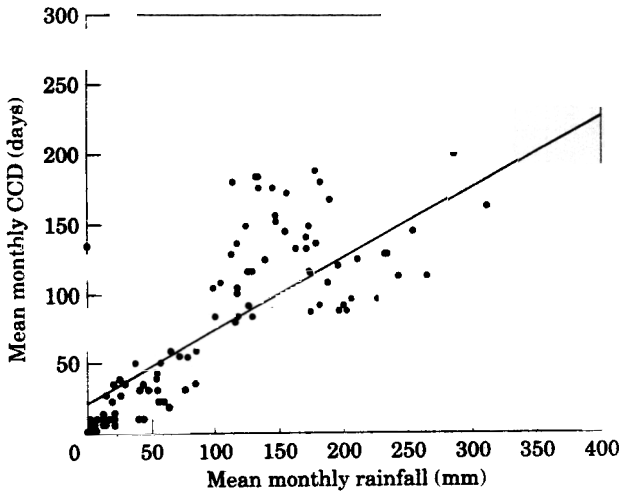


Fig. 6. The relationship between mean, monthly, cold-cloud duration (CCD) for the period 1988–1992 and mean, monthly rainfall at meteorological stations in Côte d'Ivoire and Burkina Faso for the period 1941–1971 ( $r^2=0.61$ ;  $n=132$ ;  $P \leq 0.001$ ).

#### CURRENT DATA AVAILABILITY

The five-channel, GAC data-set derived from the NOAA AVHRR is unique in its daily global coverage. It has been archived since 1981 and has been used by a wide variety of disciplines (Huh, 1991; Ehrlich *et al.*, 1994;

Townshend, 1994). These data are presently being re-processed to an  $8 \times 8$  km resolution product of both daily and dekadal composite images, as part of the NASA/NOAA path-finder project (Maiden and Greco, 1994). They are freely available to the scientific community from Goddard DAAC User Services

Office, Global Change Data Center Code 902-2, NASA, Goddard Space Flight Center, Greenbelt, MD 20771, U.S.A. (e-mail: daacuso@daac.gsfc.nasa.gov) (James and Kalluri, 1994). Many of the problems of satellite-sensor drift, of image registration to maps, of removal of cloud contamination and of inter-satellite calibration have been addressed before and during re-processing of the pathfinder products. Ancillary information stored with each image (as additional data layers) includes cloud-cover estimates, satellite view angle and Sun angle data (Agbu and James, 1994). These data will allow end-users to check and manipulate image quality and derive their own data products. The pathfinder data are being registered to a composite map projection, the Goode's homolosine projection, which ostensibly combines the advantages of the sinusoidal projection for lower latitudes (from the equator to  $\pm 40^\circ 44'11.8''$ ) and the Mollweide projection for higher latitudes, to both poles (Snyder, 1987). Because different centres of projection are used for different parts of the World (thereby locally retaining the advantages of minimal scale distortion near the centres of projection), the resulting global map looks like segments of orange peel removed from an orange. Details of the pathfinder implementation of this map projection are given in Steinwand (1994).

Meteosat CCD imagery is currently produced by the ARTEMIS programme and images are available only through collaborative links with the research programme. Raw Meteosat data is also commercially available from the European space operations centre (ESOC; Robert-Boschstrasse 5, 6100 Darmstadt, Germany) of EUMETSAT (European Organization for the Exploitation of Meteorological Satellites).

## FUTURE SPACE PLATFORMS

For remotely sensed data to become routinely used in vector monitoring and as an integral part of subsequent management procedures, it is important to know for how long we can expect to receive such imagery, to what extent the user community will have access and what

improvements might reasonably be expected in the near future.

Data should be available until the year 2000 from the present Meteosat satellites and a future Meteosat-7 satellite scheduled for launch at the end of 1995 (Schmetz, 1995). Subsequent to this, the Meteosat second generation (MSG) satellites will come into operation. These satellites will carry a new radiometer, the spinning enhanced visible and infra-red imager (SE-VIRI), which will provide  $1 \times 1$  km resolution images, every 15 min, in 12 channels ranging from  $0.5 \mu\text{m}$  in the visible region to  $13.4 \mu\text{m}$  in the infra-red domain (Schmetz, 1995).

Continuity of data from the NOAA AVHRR, polar-orbiting satellites is guaranteed both in the short term, by the successful launch of NOAA 14 in December 1994, and in the longer term, as plans have been published for a further six NOAA satellites in collaboration with the U.S. Department of Defense (Power, 1995). These new satellites will have slightly modified specifications, the AVHRR channel 3 being split into a  $1.6\text{-}\mu\text{m}$  channel in the daylight phase of the orbit and remain in its original  $3.55\text{-}3.93\text{-}\mu\text{m}$  configuration during the night-time phase (Mandt, 1995).

Superseding and complementing these instruments are the next generation of NASA Earth-observing-system (EOS) satellites, constructed with the objective of producing 'a regular global dataset of well calibrated data of high radiometric resolution for a wide array of Earth system sciences' (Running *et al.*, 1994). They will have an on-board, moderate-resolution, imaging spectroradiometer (MODIS) with 36 channels spanning the spectral range  $0.415\text{-}14.235 \mu\text{m}$ , spatial resolutions of between 250 m and 1 km, and a repeat time of 16 days (Asrar and Dokken, 1993). The EOS satellite carrying MODIS is scheduled for launch in 1998.

It is proposed that various outputs, including more accurate vegetation indices and land-surface-temperature products, will be provided, together with a range of biophysical variables and details such as the extent and processes of change in land cover. It is an aim that the data will be collected and disseminated rapidly via the internet, giving previously unparalleled access to contemporary data on

large-area, ecosystem processes (Running *et al.*, 1994). For a general perspective and review on present initiatives to archive and disseminate remotely sensed data of the land surface see Justice *et al.* (1995).

## CONCLUSIONS

The potential for using satellite surrogates of meteorological data over large areas in the study of the distribution and abundance of arthropod vectors is highlighted. Current, passive satellite systems can offer the epidemiologist insight into a variety of meteorological parameters important in determining the characteristics of the life histories of these vectors. It is necessary to stress that this information can be geographically extensive and is archived globally from the early 1980s to the present, allowing the study of large-area ecological phenomena and their changes through time. The intelligent application of such satellite data has particular potential in tropical areas, where the resources and infrastructure are such that ground data cannot be obtained. The satellite data are readily and freely available to scientists through NASA/NOAA pathfinder projects and are becoming increasingly accessible to epidemiologists as

computing power and storage facilities become cheaper in real terms. Finally, future satellite systems dedicated to measuring land-surface parameters offer many new challenges and opportunities for the objective assessment and monitoring of meteorological variables and thus vector distributions and abundance in real time.

**ACKNOWLEDGEMENTS.** It remains to thank the members of the Trypanosomiasis and Land-use in Africa (TALA) research group who have contributed in various ways to the above work, particularly Drs S. Randolph, D. Bourn and W. Wint. The channel-4 brightness temperature data were supplied by the Global Inventory Monitoring and Modelling Systems (GIMMS) group at the National Aeronautics and Space Administration, Goddard Space Flight Centre (GSFC), for work towards a NASA Planetary Biology Internship to S.I.H. The Meteosat data were kindly supplied by F. Sniijders of the ARTEMIS project at FAO, Rome. Thanks are also due to A. Mills and S. Norris for comments on early drafts of the manuscript. This work is funded by a grant from the Overseas Development Administration (ODA; R5794) administered through the Natural Resources Institute (NRI).

## REFERENCES

- AGBU, P. A. & JAMES, M. E. (1994). *The NOAA/NASA Pathfinder AVHRR Land Data Set User's Manual*. Goddard Space Flight Centre, MD: National Aeronautics and Space Administration.
- ANON. (1983). *Tables of Temperature, Relative Humidity, Precipitation and Sunshine for the World, Part 4*. London: Her Majesty's Stationery Office.
- ANON. (1994). *ARTEMIS: Africa Real Time Environmental Monitoring and Information System*. Accra, Ghana: Food and Agricultural Organization.
- ASRAR, G. & DOKKEN, D. J. (1993). *EOS Reference Handbook*. Goddard Space Flight Centre, MD: National Aeronautics and Space Administration.
- BALDWIN, D. & EMERY, W. J. (1993). Systematized approach to AVHRR navigation. *Annals of Glaciology*, 17, 414-420.
- BARRETT, E. C. & CURTIS, L. F. (1992). *Introduction to Environmental Remote Sensing*, 3rd Edn. London: Chapman & Hall.
- BELWARD, A. S. (1992). Spatial attributes of AVHRR imagery for environmental monitoring. *International Journal of Remote Sensing*, 13, 193-208.
- BELWARD, A. S. & LAMBIN, E. (1990). Limitations to the identification of spatial structures from AVHRR data. *International Journal of Remote Sensing*, 11, 921-927.
- BURSELL, E. (1957). The effect of humidity on the activity of tsetse flies. *Journal of Experimental Biology*, 34, 42-51.

- BURSELL, E. (1958). The water balance of tsetse pupae. *Philosophical Transactions of the Royal Society of London, Series B*, 241, 179–210.
- BURSELL, E. (1959). The water balance of tsetse flies. *Transactions of the Royal Entomological Society of London*, 111, 205–235.
- BUXTON, P. A. & LEWIS, D. J. (1934). Climate and tsetse flies, laboratory studies upon *Glossina submorsitans* and *tachinoides*. *Philosophical Transactions of the Royal Society of London, Series B*, 224, 175–240.
- CLINE, B. L. (1970). New eyes for epidemiologists, aerial photography and other remote sensing techniques. *American Journal of Epidemiology*, 92, 85–89.
- COLWELL, J. E. (1974). Vegetation canopy reflectance. *Remote Sensing of Environment*, 3, 175–183.
- COLWELL, R. N. (1983). *Manual of Remote Sensing*. Falls Church, VA: American Society of Photogrammetry.
- COOPER, D. I. & ASRAR, G. M. (1989). Evaluating atmospheric correction models for retrieving surface temperatures from the AVHRR over a tallgrass prairie. *Remote Sensing of Environment*, 27, 93–102.
- CRACKNELL, A. P. & HAYES, L. W. B. (1991). *Introduction to Remote Sensing*. London: Taylor & Francis.
- CURRAN, P. J. (1985). *Principles of Remote Sensing*. London: Longman.
- DUGDALE, G., McDUGALL, V. & THORNE, V. (1995). The TAMSAT method for estimating rainfall over Africa and its implications. In *Proceedings of the 21st Annual Conference of the Remote Sensing Society*, pp. 773–780. London: Butler & Tanner.
- EHRlich, D., ESTES, J. E. & SINGH, A. (1994). Applications of NOAA-AVHRR 1 km data for environmental monitoring. *International Journal of Remote Sensing*, 15, 145–161.
- EMERY, W. J., BROWN, J. & NOWAK, Z. P. (1989). AVHRR image navigation: summary and review. *Photogrammetric Engineering and Remote Sensing*, 55, 1175–1183.
- FLASSE, S. & VERSTRAETE, M. M. (1994). Monitoring the environment with vegetation indices, comparison of NDVI and GEMI using AVHRR data over Africa. In *Vegetation, Modelling and Climate Change Effects*, eds Veroustraete, F. & Ceulemans, R. pp. 107–135. The Hague: SPB Academic.
- FLITCROFT, I. D., MILFORD, J. R. & DUGDALE, G. (1989). Relating point to average rainfall in semi-arid West Africa and implications for rainfall estimates derived from satellite data. *Journal of Applied Meteorology*, 28, 252–266.
- GORMAN, A. J. & MCGREGOR, J. (1994). Some considerations for using AVHRR data in climatological studies. II. Instrument performance. *International Journal of Remote Sensing*, 15, 549–565.
- GOWARD, S. N., WARING, R. H., DYE, D. G. & YANG, J. (1994). Ecological remote sensing at OTTER: satellite macroscale observations. *Ecological Applications*, 4, 322–343.
- HANNAN, N. P., PRINCE, S. D. & HOLBEN, B. N. (1995). Atmospheric correction of AVHRR data for biophysical remote sensing of the Sahel. *Remote Sensing of Environment*, 51, 306–316.
- HASTINGS, D. A. & EMERY, W. J. (1992). The advanced very high resolution radiometer (AVHRR): a brief reference guide. *Photogrammetric Engineering and Remote Sensing*, 58, 1183–1188.
- HAY, S. I. (1993). *An Investigation into the Utility of Raw Waveband AVHRR GAC Data in Relation to Tsetse Fly Distribution Mapping and Abundance Monitoring*. Marine Biological Laboratory Woods Hole, MA: NASA Planetary Biology Internship Program.
- HIELKEMA, J. U. (1990). Satellite environmental monitoring for migrant pest forecasting by FAO: the ARTEMIS system. *Philosophical Transactions of the Royal Society of London, Series B*, 328, 705–717.
- HOLBEN, B. N. (1986). Characteristics of maximum-value composite images from temporal AVHRR data. *International Journal of Remote Sensing*, 7, 1417–1434.
- HUETE, A. R. (1988). A soil adjusted vegetation index (SAVI). *Remote Sensing of Environment*, 25, 295–309.
- HUETE, A. R., JACKSON, R. D. & POST, D. F. (1985). Spectral response of a plant canopy with different soil backgrounds. *Remote Sensing of Environment*, 17, 37–53.
- HUGH-JONES, M. (1989). Applications of remote sensing to the identification of the habitats of parasites and disease vectors. *Parasitology Today*, 5, 244–251.
- HUH, O. K. (1991). Limitations and capabilities of the NOAA satellite advanced very high resolution radiometer (AVHRR) for remote sensing of the Earth's surface. *Preventive Veterinary Medicine*, 11, 167–183.
- HUTCHINSON, C. F. (1991). Use of satellite data for famine early warning in sub-Saharan Africa. *International Journal of Remote Sensing*, 12, 1405–1421.
- JACKSON, R. D. & HUETE, A. R. (1991). Interpreting vegetation indices. *Preventive Veterinary Medicine*, 11, 185–200.

- JAMES, M. E. & KALLURI, S. N. V. (1994). The pathfinder AVHRR land data set—an improved coarse resolution data set for terrestrial monitoring. *International Journal of Remote Sensing*, 15, 3347–3363.
- JUSTICE, C. O., BAILEY, G. B., MAIDEN, M. E., RASOOL, S. I., STREBEL, D. E. & TARPLEY, J. D. (1995). Recent data and information system initiatives for remotely sensed measurements of the land surface. *Remote Sensing of Environment*, 51, 235–244.
- JUSTICE, C. O., MARKHAM, B. L., TOWNSHEND, J. R. G. & KENNARD, R. L. (1989). Spatial degradation of satellite data. *International Journal of Remote Sensing*, 10, 1539–1561.
- JUSTICE, C. O., TOWNSHEND, J. R. G., HOLBEN, B. N. & TUCKER, C. J. (1985). Analysis of the phenology of global vegetation using meteorological satellite data. *International Journal of Remote Sensing*, 10, 1539–1561.
- KAUFMAN, Y. L. & TANRÉ, D. (1992). Atmospherically resistant vegetation index (ARVI) for EOS-MODIS. *IEEE Transactions on Geoscience and Remote Sensing*, 30, 261–270.
- KHAN, B., HAYES, L. W. B. & CRACKNELL, A. P. (1995). The effects of higher-order resampling on AVHRR data. *International Journal of Remote Sensing*, 16, 147–163.
- KIDWELL, K. B. (1995). *NOAA Polar Orbiter Data Users Guide (TIROS-N, NOAA-6, NOAA-7, NOAA-8, NOAA-9, NOAA-10, NOAA-11, NOAA-12, NOAA-13 and NOAA-14)*. Washington, D.C.: National Oceanic and Atmospheric Administration.
- KINEMAN, J., BOYLE, S. C., MEALY, A., OHRENSCHALL, M., COLBY, J. D., DELLA MANA, S. & MELLON, D. (1990). *Global Change Database Project: Pilot Project for Africa. Data Set Documentation, Version 1.0 (Dakar Workshop)*. Boulder, CO: World Data Center A for Solid Earth Geophysics, United States Department of Commerce.
- KRASNOPOLSKY, V. M. & BREAKER, L. C. (1994). The problem of AVHRR image navigation revisited. *International Journal of Remote Sensing*, 15, 979–1008.
- LENNON, J. J. & TURNER, J. R. G. (1995). Predicting the spatial distribution of climate: temperature in Great Britain. *Journal of Animal Ecology*, 64, 370–392.
- LILLESAND, T. M. & KIEFER, R. W. (1994). *Remote Sensing and Image Interpretation*, 3rd Edn. New York: John Wiley & Sons.
- LOS, S. O. (1993). Calibration adjustment of the NOAA AVHRR normalized difference vegetation index without recourse to component channel 1 and 2 data. *International Journal of Remote Sensing*, 14, 1907–1917.
- MAIDEN, M. E. & GRECO, S. (1994). NASA's pathfinder dataset programme: land surface parameters. *International Journal of Remote Sensing*, 15, 3333–3345.
- MANDT, G. (1995). NOAA polar-orbiting operational environmental satellite program: status and plans. In *Proceedings of the 1995 Meteorological Satellite Data Users' Conference*, pp. 29–35. Darmstadt: European Organization for the Exploitation of Meteorological Satellites.
- MCGREGOR, J. & GORMAN, A. J. (1994). Some considerations for using AVHRR data in climatological studies, I. Orbital characteristics of NOAA satellites. *International Journal of Remote Sensing*, 15, 537–548.
- MILFORD, J. R. & DUGDALE, G. (1990). Monitoring of rainfall in relation to the control of migrant pests. *Philosophical Transactions of the Royal Society of London, Series B*, 328, 689–704.
- MONTEITH, J. L. & UNSWORTH, M. H. (1990). *Principles of Environmental Physics*, 2nd Edn. London: Edward Arnold.
- MYNENI, R. B., HALL, F. G., SELLERS, P. J. & MARSHAK, A. L. (1995a). The interpretation of spectral vegetation indexes. *IEEE Transactions on Geosciences and Remote Sensing*, 33, 481–486.
- MYNENI, R. B., MAGGION, S., IAQUINTA, J., PRIVETTE, J. L., GOBRON, M., PINTY, B., KIMES, D. S., VERSTRATE, M. M. & WILLIAMS, D. L. (1995b). Optical remote sensing of vegetation: modelling caveats and algorithms. *Remote Sensing of Environment*, 51, 169–168.
- NASH, T. A. M. (1933). A statistical analysis of the climatic factors influencing the density of tsetse flies, *Glossina morsitans* Westw. *Journal of Animal Ecology*, 2, 197–203.
- NASH, T. A. M. & PAGE, W. A. (1953). The ecology of *Glossina palpalis* in northern Nigeria. *Transactions of the Royal Entomological Society of London*, 104, 71–169.
- NORMAN, J. M., DIVAKARLA, M. & GOEL, N. S. (1995). Algorithms for extracting information from remote thermal-IR observations of the Earth's surface. *Remote Sensing Environment*, 51, 157–168.
- PETTY, G. W. (1995). The status of satellite based rainfall estimation over land. *Remote Sensing of Environment*, 51, 125–137.

- PFIRMAN, E. S. (1991). *IDA, Image Display and Analysis Version 4.0, User's Guide*. Arlington, VA: USAID Famine Early Warning System Project.
- PINTY, B. & VERSTRAETE, M. M. (1992). GEMI, a non-linear index to monitor global vegetation from satellites. *Vegetatio*, **101**, 15–20.
- PLATT, R. B., LOVE, G. J. & WILLIAMS, E. L. (1958). A positive correlation between relative humidity and the distribution and abundance of *Aedes vexans*. *Ecology*, **39**, 167–169.
- POWER, C. (1995). NOAA 14 is successfully launched. *Remote Sensing Society Newsletter*, **81**, 2.
- PRABHAKARA, C., DALU, G. & KUNDE, V. G. (1974). Estimation of sea surface temperature from remote sensing in the 11- to 13- $\mu\text{m}$  window region. *Journal of Geophysical Research*, **79**, 5039–5044.
- PRATA, A. J. (1993). Land surface temperatures derived from the advanced very high resolution radiometer and the along-track scanning radiometer I. Theory. *Journal of Geophysical Research*, **98**, 16 689–16 702.
- PRICE, J. C. (1984). Land surface temperature measurement for the split window channels of the NOAA 7 advanced very high resolution radiometer. *Journal of Geophysical Research*, **89**, 7231–7237.
- PRINCE, S. D., JUSTICE, C. O. & LOS, S. O. (1991). *Remote Sensing of the Sahelian Environment: a Review of the Current Status and Future Prospects*. Ispra, Italy: Joint Research Centre, Commission of the European Communities.
- ROBINSON, T. P. (1996). Spatial and temporal resolution of coarse resolution products of NOAA-AVHRR NDVI data. *International Journal of Remote Sensing*, in press.
- ROGERS, D. J. (1988). The dynamics of vector-transmitted diseases in human communities. *Philosophical Transactions of the Royal Society of London, Series B*, **321**, 513–539.
- ROGERS, D. J., HAY, S. I. & PACKER, M. J. (1996). Predicting the distribution of tsetse fly species in West Africa using meteorological satellite data. *Annals of Tropical Medicine and Parasitology*, **90**, in press.
- ROGERS, D. J. & RANDOLPH, S. E. (1986). Distribution and abundance of tsetse flies (*Glossina* Spp.). *Journal of Animal Ecology*, **55**, 1007–1025.
- ROGERS, D. J. & RANDOLPH, S. E. (1991). Mortality rates and population density of tsetse flies correlated with satellite imagery. *Nature*, **351**, 739–741.
- RUNNING, S. W., JUSTICE, C. O., SALMONSON, V., HALL, D., BARKER, J., KAUFMAN, Y. J., STRAHLER, A. H., HUETE, A. R., MULLER, J. P., VANDERBILT, V., WAN, Z. N., TEILLET, P. & CARNEGIE, D. (1994). Terrestrial remote sensing science and algorithms planned for EOS/MODIS. *International Journal of Remote Sensing*, **15**, 3587–3620.
- SCHMETZ, J. (1995). Meteorological products from current and future EUMETSAT satellite systems. In *Proceedings of the 1995 Meteorological Satellite Data Users' Conference*, pp. 233–240. Darmstadt: European organization for the Exploitation of Meteorological Satellites.
- SELLERS, P. J. (1985). Canopy reflectance, photosynthesis and transpiration. *International Journal of Remote Sensing*, **6**, 1335–1372.
- SNIJDERS, F. L. (1991). Rainfall monitoring based on Meteosat data—a comparison of techniques applied to the Western Sahel. *International Journal of Remote Sensing*, **12**, 1331–1347.
- SNYDER, J. P. (1987). *Map Projections—a Working Manual*. U.S. Geological Survey Professional Paper 1395. Washington, D.C.: United States Government Printing Office.
- STEINWAND, D. R. (1994). Mapping raster imagery to the interrupted Goode homolosine projection. *International Journal of Remote Sensing*, **15**, 3463–3471.
- SWAIN, P. H. & DAVIS, S. M. (1978). *Remote Sensing: the Quantitative Approach*. New York: McGraw & Hill.
- TANRE, D., HOLBEN, B. N. & KAUFMAN, Y. (1992). Atmospheric correction algorithm for NOAA-AVHRR products: theory and application. *IEEE Transactions on Geoscience and Remote Sensing*, **30**, 231–248.
- TOWNSEND, J. R. G. (1994). Global data sets for land applications from the advanced very high resolution radiometer: an introduction. *International Journal of Remote Sensing*, **15**, 3319–3332.
- TUCKER, C. J. (1979). Red and photographic infrared linear combinations for monitoring vegetation. *Remote Sensing of Environment*, **8**, 127–150.
- TUCKER, C. J., NEWCOMB, W. W., LOS, S. O. & PRINCE, S. D. (1991). Mean and inter-year variation of growing-season normalized difference vegetation index or the Sahel 1981–1989. *Remote Sensing of Environment*, **8**, 127–150.
- TUCKER, C. J. & SELLERS, P. J. (1986). Satellite remote sensing of primary production. *International Journal of Remote Sensing*, **7**, 1395–1416.

- TUCKER, C. J., TOWNSHEND, J. R. G. & GOFF, T. E. (1985). African land-cover classification using satellite data. *Science*, **227**, 369–375.
- TUCKER, C. J., VANPRAET, C., BOERWINKEL, E. & GASTON, A. (1983). Satellite remote sensing of total dry matter production in the Senegalese Sahel. *Remote Sensing of Environment*, **13**, 461–474.
- UNWIN, D. M. (1980). *Microclimate Measurement for Ecologists*. Biological Techniques Series 3. London: London.
- VERMOTE, E., TANRE, D. & HERMAN, M. (1990). Atmospheric effects on satellite imagery, correction algorithms for ocean color or vegetation monitoring. *International Society for Photogrammetry and Remote Sensing*, **28**, 46–55.
- VIOVY, N., ARINO, O. & BELWARD, A. S. (1992). The best index extraction slope (BISE): a method for reducing noise in NDVI time-series. *International Journal of Remote Sensing*, **13**, 1585–1590.
- VOGT, J. (1992). *Characterising the Spatio-temporal Variability of Surface Parameters from NOAA AVHRR Data: a Case Study for Southern Mali*. Ispra, Italy: Joint Research Centre, Institute for Remote Sensing Applications.
- WASHINO, R. K. & WOOD, B. L. (1994). Application of remote-sensing to arthropod vector surveillance and control. *American Journal of Tropical Medicine and Hygiene*, **50** (Suppl.), 134–144.
- WILLMER, P. G. (1982). Microclimate and the environmental physiology of insects. *Advances in Insect Physiology*, **16**, 1–57.
- WILLMER, P. G. & UNWIN, D. M. (1981). Field analysis of insect heat budgets: reflectance, size and heating rates. *Oecologia*, **50**, 250–255.